Polygenic adaptation, clonal interference, and the evolution of mutators in experimental *Pseudomonas aeruginosa* populations

Katrina B. Harris[1], Kenneth M. Flynn[2], and Vaughn S. Cooper[1]

[1]Department of Microbiology and Molecular Genetics, and Center for Evolutionary Biology and Medicine, University of Pittsburgh, Pittsburgh, Pennsylvania, USA.

[2]Department of Molecular, Cellular, and Biomedical Sciences, University of New Hampshire, Durham, NH, USA.

Abstract:

In bacterial populations, switches in lifestyle from motile, planktonic growth to surface-grown biofilm is associated with persistence in both infections and non-clinical biofilms. Studies have identified the first steps of adaptation to biofilm growth but have yet to replicate the extensive genetic diversity observed in chronic infections or in the natural environment. We conducted a 90-day long evolution experiment with *Pseudomonas aeruginosa* PA14 in growth media that promotes biofilm formation in either planktonic culture or in a biofilm bead model. Surprisingly, all populations evolved extensive genetic diversity with hundreds of mutations maintained at intermediate frequencies, while fixation events were rare. Instead of the expected few beneficial mutations rising in frequency through successive sweeps, we observe a remarkable 40 genes with parallel mutations spanning both environments and often on coexisting genotypes within a population. Additionally, the evolution of mutator genotypes (*mutS* or *mutL* mutator alleles) that rise to high frequencies in as little as 25 days contribute to the extensive genetic variation and strong clonal interference. Parallelism in several transporters (including *pitA, pntB, nosD,* and *pchF*) indicate probable adaptation to the arginine media that becomes highly alkaline during growth. Further, genes involved in signal transduction (including *gacS*, *aer2, bdlA, and* PA14_71750) reflect likely adaptations to biofilm-inducing conditions. This experiment shows how extensive genetic and phenotypic diversity can arise and persist in microbial populations despite strong selection that would normally purge diversity.

Importance:

How biodiversity arises and is maintained in clonally reproducing organisms like microbes remains unclear. Many models presume that beneficial genotypes will outgrow others and purge variation via selective sweeps. Environmental structure like biofilms may oppose this process and preserve variation. We tested this hypothesis by evolving *P. aeruginosa* populations in biofilm-promoting media for three months and found both adaptation and diversification that were mostly uninterrupted by fixation events that eliminate diversity. Genetic variation tended to be greater in lines grown using a bead model of biofilm growth but many lineages also persisted in planktonic lines. Convergent evolution affecting dozens of genes indicates that selection acted on a wide variety of traits to improve fitness, causing many adapting lineages to co-occur and persist. This result demonstrates that some environments may expose a large fraction of the genome to selection and select for many adaptations at once, causing enduring diversity.

Introduction:

Bacterial populations inhabit countless environments along a continuum of spatial structure, ranging from a well-mixed liquid to rugged, solid surfaces. Growth on surfaces is associated with biofilm production that in turn generates nutrient and oxygen gradients (Stoodley et al. 2002; Dietrich et al. 2013), but so too does the metabolic activities of neighboring cells. Life in confined spaces results in varied levels of nutrients, waste, and signaling molecules that may alter selective forces on parts of the population and create novel ecological opportunities (Poltak and Cooper 2011). These physical differences are hypothesized to select for mutations in biofilm populations distinct from well mixed cultures. Experimental microbial evolution (EME) studies have found that biofilm populations select for different mutations than those seen in planktonic growth, and the greater environmental structure of the biofilm produces increased genetic diversity (Rainey and Travisano 1998; Boles et al. 2004; Habets et al. 2006; Wong et al. 2012; Traverse et al. 2013; Flynn et al. 2016; Santos-Lopez et al. 2019). Despite this process of diversification, replicate populations propagated in both biofilm and planktonic conditions exhibit high levels of both phenotypic and genetic parallelism, suggesting some measure of predictability within the same environment (Wong et al. 2012; Tognon et al. 2017; Yen and Papin 2017; Sanz-García et al. 2018; Turner et al. 2018). We still have much to learn about how the biofilm life cycle influences evolutionary dynamics and processes, including the relative roles of mutation and selection, and whether biofilm growth becomes the dominant selective force relative to other stresses like nutrient limitation or external toxins.

Pseudomonas aeruginosa is an opportunistic pathogen found in soil and water and is known for its ability to thrive in numerous environments. *P. aeruginosa* is a highly studied pathogen due to its association with poor outcomes in clinical settings when it forms biofilm infections within patients (Eichner et al. 2014; Feliziani, Marvig, Luján, Moyano, Di Rienzo, et al. 2014; Schick and Kassen 2018; Gloag et al. 2019). Adaptation to biofilm growth has been

indicated as a cause of infection persistence in numerous studies (Parsek and Singh 2003; Periasamy and Kolenbrander 2009; Yildiz and Visick 2009). This adaptation manifests as important colony phenotypes such as mucoidy and rugose small colony variants (RSCVs) as well as the loss of virulence factor production and altered cell surface virulence determinants (Ashish et al. 2013; Kim et al. 2014). Several studies have been performed to identify some of the first steps of adaptation to a biofilm environment but these studies have yet to replicate the high levels of genetic diversity often seen in chronic biofilm-associated infections, such as those of the airways of cystic fibrosis patients (Lieberman et al. 2011; Hogardt and Heesemann 2013; Marvig et al. 2015; Kruczek et al. 2016; Schick and Kassen 2018; Gloag et al. 2019).

We previously conducted a long-term evolution experiment over 90 days of propagation (~600 generations) to explore how the population-genetic dynamics of *P. aeruginosa* adaptation differ in a model of the biofilm life cycle compared to a well-mixed environment (Flynn et al. 2016). Major findings included that biofilm populations evolved greater phenotypic and ecological diversity than planktonic populations, and some of these phenotypes were linked to probable biofilm adaptations. The different colony types that evolved within populations represented distinct growth strategies that were most productive in mixture, suggesting a process of niche partitioning and facilitation among lineages (Flynn et al. 2016). This is strikingly opposed to the phenotypic parallelism observed in previous studies(Rainey and Travisano 1998; Traverse et al. 2013). A preliminary survey of the genomes of these lineages revealed that this diversity was in part caused by the evolution of *mutS* and *mutL* genotypes that increased mutation rate, a genotype also observed in many chronic infections of *P. aeruginosa* (Ciofu et al. 2010; Macià et al. 2011; Warren et al. 2011; López-Causapé et al. 2013). Here, we use longitudinal whole-population genome sequencing (WPGS) to study the underlying evolutionary dynamics of this experiment at high resolution. Some genes that experienced mutational parallelism contribute to arginine metabolism, the sole carbon and nitrogen source in these experiments. More surprising, in light of the duration of the experiment and the strength of

selection in these populations, few mutations actually fixed in any of the six populations and much more genetic diversity was preserved than has been seen in previous evolution experiments. We discuss potential evolutionary and phenotypic causes for this maintenance of such levels of high genetic diversity.

Results:

Experimental evolution

Six populations of *P. aeruginosa* strain PA14 (PA), a strain already proficient in forming biofilm, were propagated for 90 days (approximately 600 generations, or ~6.6 generations per day) to examine the population-genetic dynamics of prolonged growth in a biofilm life cycle. Bacteria that attach to a polystyrene bead are transferred daily to a new tube containing a fresh bead (populations B1, B2, B3), and compared to passages of serial 1:100 dilutions (planktonic populations P1, P2, P3) as described previously (Poltak and Cooper 2011; Flynn et al. 2016) (Figure S1). Biofilm and planktonic populations were designed to ensure a similar transfer size and number of generations per day, as reported previously(Flynn et al. 2016). The culture medium was M63 media containing arginine as the sole carbon and nitrogen source and supplemented with 25 μM iron (see methods), a combination which has been shown to promote biofilm production in *Pseudomonas* species (Bernier et al. 2011). We hypothesized that this media would allow us to bypass many known first-step adaptive mutations, and instead allow us to look at the subsequent steps of adaptation that are less known. We sought to study these population wide adaptations at both phenotypic and genetic levels.

After 90 days, all six populations became vastly more fit than ancestral PA14, with selective coefficients 10-fold greater (*r* between 3 and 5; see methods for selection calculation) than the fitness gains observed in other evolution experiments of similar duration (Lenski et al. 1991; Rainey and Travisano 1998; Barrett et al. 2005; Ellis et al. 2012; Wong et al. 2012) (Figure S2, Table S1; see methods). Five populations increased their maximum growth rate

(Vmax; Figure S3a) and five populations evolved to become less motile than the ancestor (Figure S3b). Despite selection to attach to a plastic bead each day, presumably by producing biofilm, only the B3 population evolved higher biofilm production than the ancestor as measured by the standard crystal violet assay. In contrast, four populations, including bead populations B1 and B2, evolved lower biofilm production (Figure S3c). This result may reflect the high starting biofilm production of PA14 in these conditions being difficult to improve. We performed a principal component analysis on these three phenotypes (Figure 1a) and found that evolved populations were distinguished from the ancestor but not clearly separated by treatment.

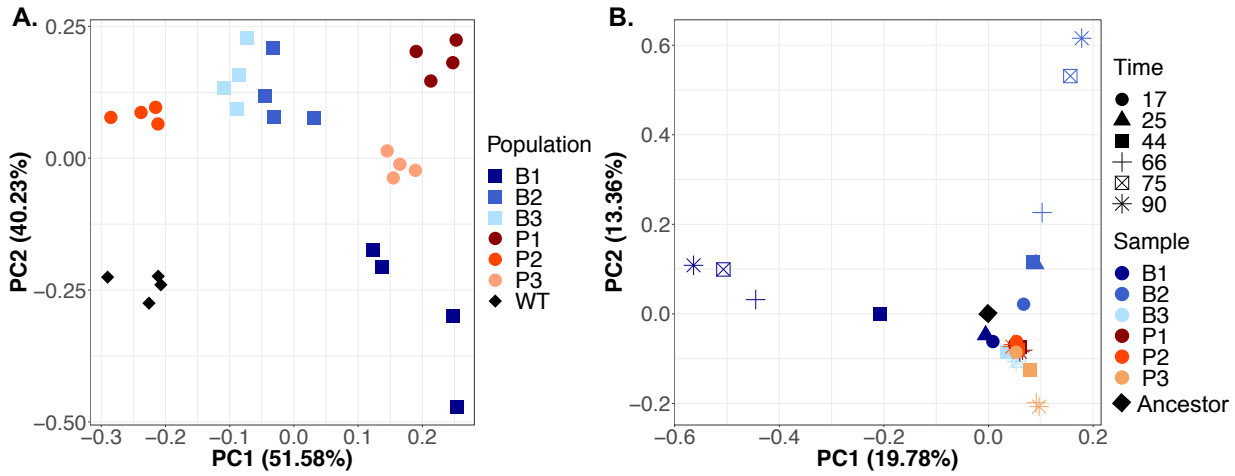

Figure 1. Divergent phenotypes linked to fitness and genotypes distinguish each evolved population after 90 days of passage. (A) PCA of evolved phenotypes including biofilm production, maximum growth rate (Vmax), and swimming motility (n = 4 for each population). Blue squares are biofilm populations, red circles are planktonic populations, and the ancestor is indicated by black diamond(s). The first three components explain 51.58%, 40.23%, and 8.19% of variance. (B) PCA of mutation identities and frequencies at Days 17, 25, 44, 66, 75, and 90. Replicate data points for each population are indicated in color. Colors are the same as in A, but shape indicates time through the experiment. The top four components explain 19.78%, 13.36%, 9.31%, and 6.5% of the variance.

High genetic diversity arose and persisted in all populations

We used longitudinal WPGS to characterize the genetic diversity and evolutionary dynamics of each lineage with an average depth of 617.1± 142.3 reads per sample. A total of 145.7 ± 55 mutations were detected per population over the course of the 90-day time period (see methods for filtering criteria). Biofilm populations accumulated more mutations (535, with 382 found at day 90) over the 90 days than planktonic populations (339, with 201 found at day 90; Table 1). This number of mutations is remarkable in comparison to previous evolution experiments. For example, *Burkholderia cenocepacia* populations were propagated using the same bead model, for twice the transfer days, and 37 mutations were identified in the best-studied population (Traverse et al. 2013). Biofilm populations were sampled at two more time points than planktonic allowing for a more accurate representation of their complex dynamics, discussed more below.

Total cumulative mutations	**874**
Biofilm only	535
Planktonic only	339
Total mutations at day 90	**583**
Biofilm only	382
Planktonic only	201
Total fixed mutations	**53**
Biofilm only	48
Planktonic only	5
Total fixation events	**10**

Table 1. Summarized mutation statistics from all six populations following 90 days of experimental evolution.

A known phenomenon associated with positive selection is the increase in nonsynonymous (NS) mutations over synonymous (S) mutations (Kryazhimskiy and Plotkin 2008; Lieberman et al. 2011). In following with this trend, the normalized NS/S ratio for planktonic populations averaged 1.73 and for biofilm populations 2.34. A total of 31 indels were also identified in the six evolved populations (Table S2, Table S3) while, interestingly, no large structural variants were detected. A large number of intergenic mutations were also identified (233 mutations, or 27.5%), many in likely promoter or terminator regions. The importance of intergenic mutations still remains unclear, however recent work has implicated intergenic regulatory regions as critical in *Pseudomonas aeruginosa* evolution in the laboratory and during infections (Feliziani, Marvig, Luján, Moyano, Rienzo, et al. 2014; Khademi et al. 2019).

We hypothesized that the structured biofilm environment would maintain greater genetic diversity than mixed liquid culture, but this ecological process is potentially at odds with the diversity-purging effect of selection on beneficial mutations. For example, a mutation that generally improves growth would be expected to sweep and eliminate genetic variation, even though the biofilm growth is predicted to increase the probability of coexisting subpopulations (Habets et al. 2006; Traverse et al. 2013; Martin et al. 2016). Planktonic populations would also be subject to similar effects of selective sweeps but their admixture might limit the cooccurrence of contending mutations (Lang et al. 2013). To summarize, comparing populations at a given time point might not adequately capture the longitudinal ecological and evolutionary dynamics affecting diversity. For this reason, we sampled biofilm populations at six time points (17, 25, 44, 66, 75, and 90 days) and planktonic populations at four time points (17, 44, 66, and 90 days) and focused on temporal changes in all mutations supported by three reads on each of both strands.

The nucleotide diversity of biofilm populations tended to be greater at the end of the experiment than after only 17 transfers (day 17 vs day 90: $p = 0.0478$, $t = 2.821$, $df = 4$ via two tailed t-test). Planktonic populations continued to select for new mutations throughout the

184 experiment, but they did not become more diverse by day 90 than at day 17 ($p = 0.239$, $t =$
185 1.384, $df = 4$ via two tailed t-test), indicating a process where new mutations were displacing
186 older ones. Biofilm populations also tended toward greater diversity than planktonic populations
187 later in the experiment, albeit not significantly (planktonic vs biofilm, day 90, $p = 0.0749$, $t =$
188 2.394, $df = 4$ via two tailed t-test; Figure S4a). These findings are consistent with the greater
189 morphological variation in biofilm populations than planktonic ones that we reported previously
190 (Flynn et al. 2016).

191 A major cause of the high genetic diversity is the prevalence of mutator alleles,
192 mutations that cause a genome-wide increase in mutation rate, in four populations. In all biofilm
193 populations and one planktonic population (P3) NS mutations in the DNA mismatch repair
194 (MMR) genes *mutS* and *mutL* became frequent or fixed. Two populations, B1 and B2,
195 independently evolved the same *mutS* mutation (T112P) that has been shown to lower affinity
196 for heteroduplex DNA in *E. coli*(Junop et al. 2003) and results in a 116-fold increase in mutation
197 rate in isogenic mutants (Figure S5). Interestingly, this T112P mutation occurs within a
198 homopolymeric region that may be a mutational hotspot. Genotypes containing these mutations
199 fix in populations B1 and B2 by days 44 and 25, respectively (Figure 2, red trajectories). A
200 premature stop mutation (W307*) in *mutS* also rose to intermediate frequency (53%) in the P3
201 population by day 90. While we did not create an isogenic mutant of this mutator allele, we
202 predict that it acts as other *mutS* mutations with a roughly 100-fold increase in mutation rate.
203 The rise of *mutS* alleles caused these populations to diverge genetically from the others, as
204 seen from PCA analysis of mutational frequency data (Figure 1B). A fourth mutator genotype
205 evolved in the B3 population by a mutation in *mutL* (D467G) that caused a 16-fold increase in
206 mutation rate and rose to 83% frequency by day 90 (Figure 2; Figure S5). Consequently, each
207 of these mutator populations became enriched for transition and single-base indel mutations,
208 signatures typical of defects in mismatch repair (Sniegowski et al. 1997; Shaver et al. 2002;
209 Couce et al. 2017) (Table S2).

210 .

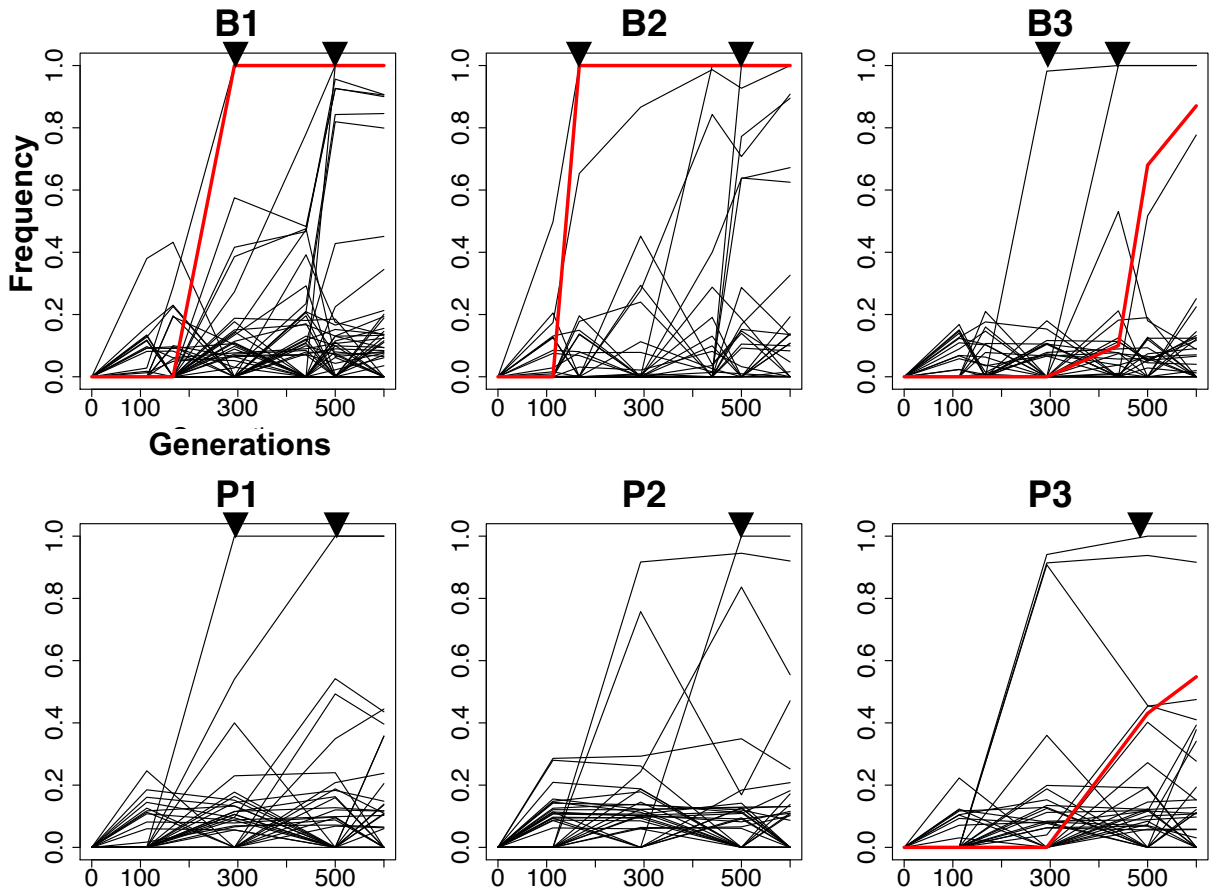

211

212 **Figure 2.** Evolutionary trajectories of inferred genotypes within six PA populations under biofilm
213 (B) or planktonic (P) selection. Genotypes containing mutator alleles are colored red. Triangles
214 indicate timing of the ten fixation events observed throughout the study.
215
216

High diversity is a byproduct of clonal interference

While mutator alleles are not beneficial themselves (Sniegowski et al. 1997) and their dominant effect is to introduce neutral or deleterious mutations, they can facilitate the acquisition of combinations of beneficial mutations. A more beneficial genotype that has acquired several beneficial mutations may be able to outcompete less fit lineages with fewer mutations and overcome competition among adaptive lineages that slows their rate of increase. This dynamic is known as clonal interference or more generally as the Hill-Robertson effect (Birky and Walsh 1988; McVean and Charlesworth 2000; Comeron et al. 2008). The ability to acquire many beneficial mutations and escape clonal interference may be particularly advantageous when beneficial genetic variation is rare or, more likely in these populations, common (Smith and Haigh 1974; Buskirk et al. 2017).

As described above, hundreds of mutations rose to detectable frequencies in these populations within ~200 generations and persisted. We used software recently developed by our lab to group mutations into genotypes on the basis of shared, nested frequency-trajectories (cdeitrick 2020). Remarkably, between 30 and 47 genotypes each composed of multiple mutations accumulated within each population throughout the experiment (Figure 2). The number of genotypes present at a given sampled timepoint continuously increased in biofilm populations, whereas the maximum diversity in planktonic populations occurred at day 44 (Supplemental Figure 4). Yet despite extensive variation at both nucleotide and genotype levels, only 10 fixation events were observed involving a total of 53 mutations. These selective sweeps involved genotypes with more mutations in biofilm populations than in planktonic lines (Table 1), and two sweeps were linked to mutator alleles in which 24 mutations fixed (Table S3). These results suggest that the biofilm environment selected larger mutational cohorts that could involve more differentiated genotypes to fix, whereas planktonic populations selected one or few mutations to fix. One cause of this pattern was the superiority of mutator genotypes containing more linked mutations, which were more common in biofilm lines. Combined, these findings

suggest that the rapid rise of mutator alleles may have enabled escape from clonal interference, especially in biofilms.

To better understand the evolutionary processes within these populations, we visualized genotype frequencies over time by constructing Muller plots (Traverse et al. 2013; Scribner et al. 2019). These figures demonstrate, for example, how one genotype spreads by evolving secondary, nested, genotypes and outcompeting other preexisting genotypes. The most conspicuous genotype invasions were the mutator genotypes in populations B1 and B2 containing 11 or 13 mutations (Figure 3; mutator ancestry depicted in color and fixation events depicted by vertical lines). These figures also illustrate effects of particularly consequential mutations that overtake others or give rise to further diversity as well as genotypes that arise simultaneously and coexist for hundreds of generations. This latter dynamic is consistent with either clonal interference or genotypes adapting to inhabit discrete niches, possibilities we evaluate below.

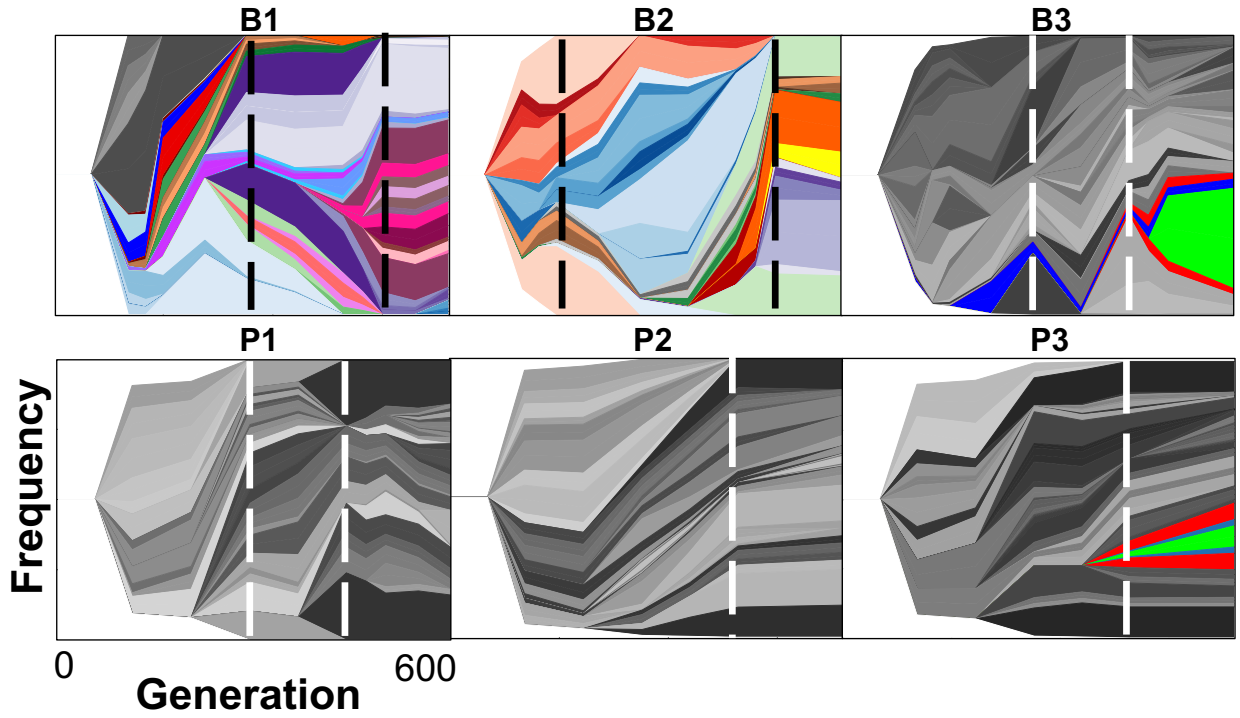

Figure 3. Genealogy and genotype frequencies over time. Each shade or color represents a different genotype and vertical area corresponds to genotype frequency, inferred by LOLIPop (cdeitrick 2020). Shades of grey indicate genotypes not on a mutator background, whereas colors indicate genotypes on a mutator background. Dashed lines indicate timing of fixation events predicted by genotype trajectories (Figure 2). Biofilm populations are on the top row and planktonic populations are on the bottom row.

To test the genotype prediction algorithm producing these Muller plots and to identify other mutations undetected due to their low frequencies or sequencing coverage, we sequenced 26 clones from population B1 and 10 from population P1. B1 clones contained 48-138 mutations per clone whereas clones from the P1 population only contained between 14-28 mutations, results consistent with population sequencing results. However, many of these mutations were previously undetected in the metagenomes, indicating much greater genetic variation at frequencies below our detection limits from population sequencing (Figure 4) (Good et al. 2017). The 26 B1 clones belonged to a total of nine competing genotypes at day 90 (Figure S6), whereas the 10 planktonic clones only belonged to two distinct genotypes (Figure S7). This finding confirms that the biofilm population maintained greater genetic diversity than the planktonic population at the end of the experiment.

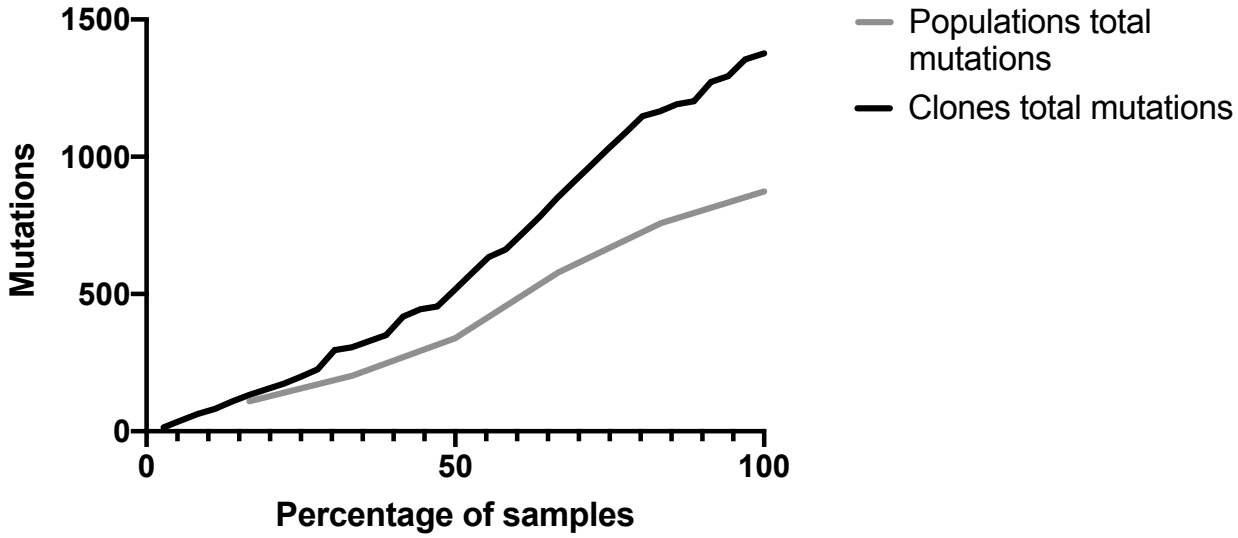

Figure 4. Clonal sequencing identifies more mutational variation than population level sequencing. Collector's curve of total mutations identified by both population and clonal sequencing. To enable comparison results are plotted by the percentage of samples obtained (6 populations or 36 clones).

Another goal of sequencing these clones was to determine the genetic causes of the distinct colony morphologies that we previously showed to associate with distinct niches and phenotypes within the B1 biofilm population (Flynn et al. 2016). Each of the seven morphotypes (Figure 5a) represented a different long-lived genetic lineage (Figure 5b) that was separated by at least five mutations. This indicates the previous study that was based solely on colony morphotypes captured a good representation of the population diversity as it included seven of nine identified genotypes. We examined mutations unique to each genotype in an effort to identify those responsible for their unique phenotypes, which included the ability to form more productive biofilm communities in mixture (Table 2).

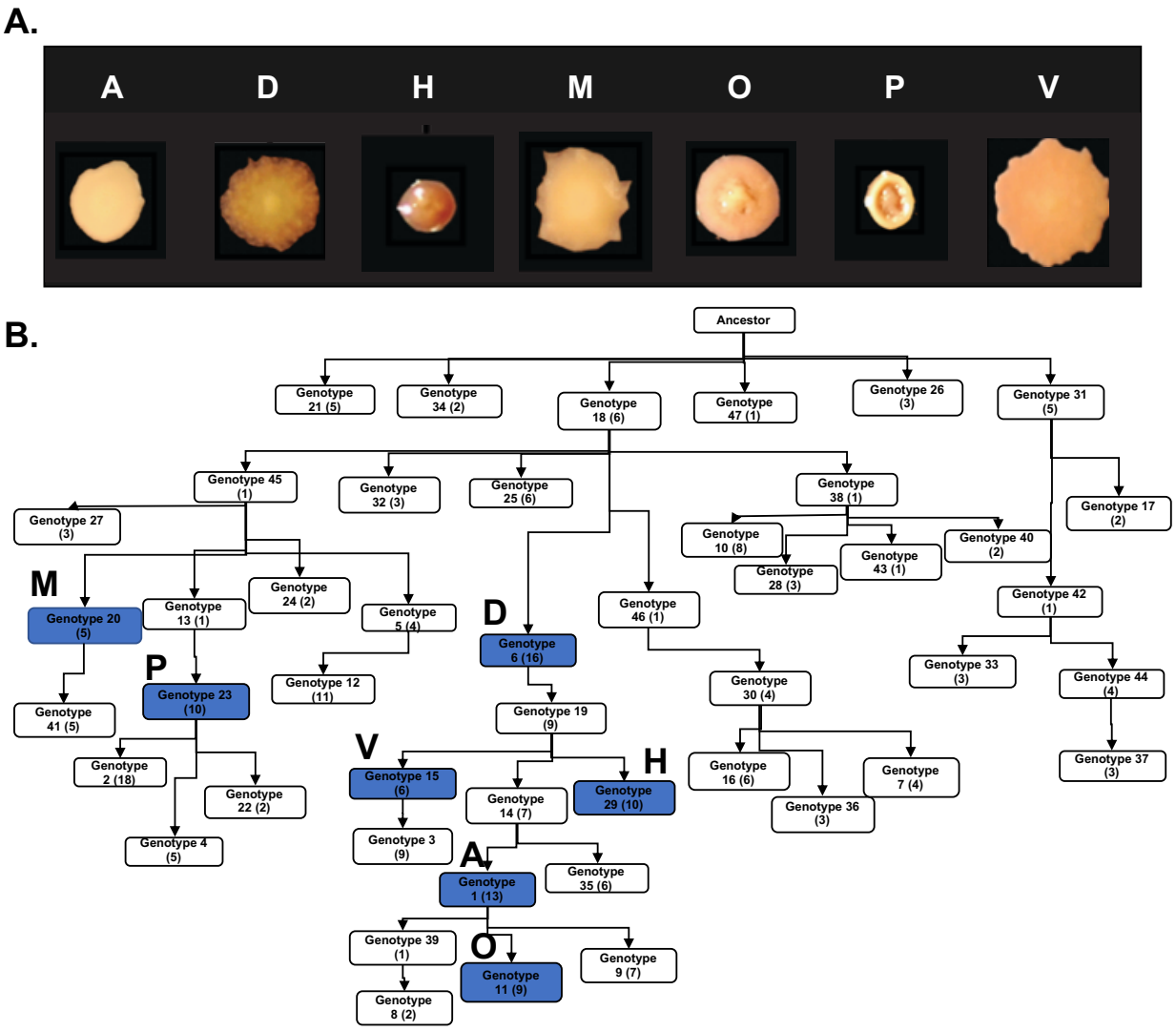

Figure 5. Clones representing different colony morphologies from the B1 population are all at different points on the evolutionary trajectory of the B1 population. (A) Seven colony morphologies were identified at day 90 and their phenotypes and ecological interactions were characterized previously(Flynn et al. 2016). (B) Ancestry was inferred using LOLIPop (cdeitrick 2020). Genotypes of named morphotypes are shown in blue.

For five morphotypes we can predict a genetic cause of the high biofilm formation and the related high c-di-GMP levels. Morphotypes A and H each independently acquired mutations in *gacS*, a sensor kinase known to be associated with high biofilm production(Davies et al. 2007), and which will be discussed more below. The additional three evolved mutations in separate genes that have all been linked to *Pseudomonas* biofilm production previously: mutant

303 D acquired a mutation in the sensor histidine kinase *rcsC* (Nicastro et al. 2009), M acquired a
304 mutation in the type III secretion system gene *pscQ* (Wagner et al. 2003), and V acquired a
305 mutation in the two component response regulator PA14_52250 (Francis et al. 2017; Badal et
306 al. 2020) (Table 2). While these are not the only mutations that distinguish the morphotypes
307 from one another, these are leading candidates that could produce their varied biofilm
308 phenotypes.

Clone	Gene	PA01 ortholog	Pseudocap function
A	bkdA1	bdkA1	
	flgB	flgB	Motility & Attachment
	oprC	oprC	Transport of small molecules
	oprC	oprC	Transport of small molecules
	PA14_06960	PA0534	Putative enzymes
	PA14_10830	no PA01 ortholog	Transcriptional regulators
	PA14_14530>/>PA14_14540		
	gacS	gacS	Two-component regulatory systems
	PA14_52760	PA0891	Transport of small molecules
	PA14_72320	PA5478	Membrane proteins
	ppc	ppc	Central intermediary metabolism
	thrB>/<PA14_72520		
	TrpB	TrpB	Amino acid biosynthesis and metabolism
D	oprH</>napE	oprH</>napE	
	PA14_04050	PA0227	Biosynthesis of cofactors, prosthetic groups and carriers
	PA14_06030	PA0461	Fatty acid and phospholipid metabolism
	PA14_10910	PA4096	Transport of small molecules
	PA14_19450	PA3453	Hypothetical, unclassified, unknown
	PA14_23670	PA3127	Antibiotic resistance and susceptibility
	PA14_29260	PA2696	Transcriptional regulators
	PA14_31470	PA2557	Fatty acid and phospholipid metabolism
	PA14_48210	PA1239	Putative enzymes
	PA14_55380</<PA14_55390		
	magD	magD	Adaptation, Protection

	PA14_66380	PA5021	Membrane proteins
	pauR	pauR	Carbon compound catabolism
	PA14_71750	PA5437	Transcriptional regulators
	pvdJ	pvdJ	Adaptation, Protection
H	algU</>nadB	algU</>nadB	
	dsbA2	dsbA2	Translation, post-translational modification, degradation
	gbuR	gbuR	Transcriptional regulators
	PA14_19190	PA3471	Central intermediary metabolism
	prkA	prkA	
	fliT	fliT	Motility & Attachment
	gacS	gacS	Two-component regulatory systems
	PA14_58960	no PA01 ortholog	Hypothetical, unclassified, unknown
	PA14_71750	PA5437	Transcriptional regulators
	rpoB	rpoB	Transcription, RNA processing and degradation
M	flhA	flhA	Motility & Attachment
	PA14_07810	PA0599	Hypothetical, unclassified, unknown
	PA14_13150	PA3921	Transcriptional regulators
	PA14_43150</>PA14_43160		
	pscQ	pscQ	Protein secretion/export apparatus
O	PA14_12160	PA3992	Putative enzymes
	PA14_14390</>PA14_14400		
	PA14_27610>/>PA14_27620		
	PA14_27770	PA2812	Transport of small molecules
	PA14_51510	PA0988	Hypothetical, unclassified, unknown
	pstA	pstA	Transport of small molecules
	spuF	spuF	Transport of small molecules
	str	str	Antibiotic resistance and susceptibility
	trbL	trbL	
P	lpxC	lpxC	Cell wall / LPS / capsule
	mdoH	mdoH	Cell wall / LPS / capsule
	PA14_03000	PA0242	Putative enzymes
	PA14_13140>/>PA14_13150		
	PA14_1340>/<PA14_13350		
	PA14_18760	PA3523	Transport of small molecules
	PA14_43150	PA1652	Membrane proteins

	pilF	pilF	Motility & Attachment
	purB	purB	Amino acid biosynthesis and metabolism
	rep	rep	DNA replication, recombination, modification and repair
V	rsmE	rsmE	Translation, post-translational modification, degradation
	pqiB	no PA01 ortholog	Hypothetical, unclassified, unknown
	PA14_52250	PA0929	Two-component regulatory systems
	rsmI	rsmI	Translation, post-translational modification, degradation
	thrB>/<PA14_72520		
	til5a>/>pldA		

Table 2. Unique mutations found in seven clones from an experimentally evolved biofilm populations with distinct ecological roles(Flynn et al. 2016).

Targets of selection

Evolving large populations (>10^8) over a few hundred generations results in higher impacts of selection relative to the effect of drift, even when mutation rates increase. This allows us to predict that genotypes that rise to a detectable frequency in an evolve-and-resequence experiment like this one are fitter than their ancestor. Further, parallel, nonsynonymous mutations affecting the same gene provides strong evidence of an adaptation (Cooper 2018). Across all six populations, 53 mutations reach 100% frequency, as part of the 10 genotype sweeps (Table 1), and each affected a unique gene except for two each in *mutS*, *pitA*, and *rpoB* (Table S3). However, the population dynamics depicted in Figure 3 and the clonal genomes summarized in Figure 5 demonstrate substantial genetic variation that did not fix. We suspected a more appropriate screen for parallelism might involve a lower frequency threshold than 100%. At 80% frequency, eight genes were mutated more than once: *lysC, mutS*, the intergenic region *fabI/ppiD*, PA14_23670*, pitA*, PA14_69980, PA14_71750, and *rpoB*, and all six populations are represented. Mutations affecting these genes were either small indels or nonsynonymous substitutions predicted to alter or eliminate function. Because these genes were mutated in both planktonic and biofilm environments, they likely enable adaptation to the growth medium,

328 temperature, and dilution timing. However, these represent only 17 of the 116 mutations that
329 reach 80% frequency, a remarkably flat distribution of high-frequency genotypes that suggests
330 many loci may provide a benefit under these conditions.
331 We next analyzed the complete set of parallel mutations found at all frequencies for
332 those passing a statistical threshold of expected random co-occurrence and identified 153
333 genes or intergenic regions. Forty genes were mutated three or more times, more than would be
334 expected by chance, accounting for 179 mutations (21.1% of all mutations; Table 3). Most
335 mutations are nonsynonymous, as expected from positive selection, and many suggest possible
336 adaptive phenotypes.
337 The gene with the most independent mutations, *rluB* (PA14_23110) with 10 (8
338 nonsynonymous; Table 3, Table S3) found in four populations at frequencies of 12.1-17.7%, is
339 difficult to understand as an adaptation. *RluB* encodes a 23s rRNA pseudouridine synthase
340 responsible for modifying this rRNA at position 2605 during maturation (Kaczanowska and
341 Rydén-Aulin 2007). This gene was mutated in both biofilm and planktonic populations, indicating
342 it is not specific to lifestyle, but all mutations clustered in residues 313 and 323 found in the
343 disordered C-terminus of this protein. In addition, one mutation in *rluC*, another pseudouridine
344 synthase, was detected. The literature remains vague about the specific phenotypic roles of
345 these 23S rRNA modifications and effects of disrupting these genes are difficult to detect *in*
346 *vitro*, but a recent study implicated these modifications as important for growth under anoxia
347 (Krishnan and Flower 2008; Basta et al. 2017).
348 Fortunately, a wealth of literature has identified genes involved in the transition from
349 planktonic to biofilm growth in *P. aeruginosa* (Boles et al. 2004; Eichner et al. 2014). These
350 genes are often well annotated at http://pseudomonas.com for the PA14 genome or in related
351 strains (Winsor et al. 2016). For example, five mutations in PA14_02220, encoding the aerotaxis
352 transducer Aer2, were selected in two biofilm and one planktonic population, and may alter the
353 response to low oxygen that is common in biofilms (Sawai et al. 2012). In addition, three

354 independent V334G mutations were selected in each biofilm population in PA14_46030,
355 encoding the ortholog of biofilm dispersion locus BdlA (Morgan et al. 2006). This cytoplasmic
356 protein contains two sensory PAS domains and a chemoreceptor domain that has been shown
357 to sense and mediate responses to oxygen levels (Petrova and Sauer 2016). Two-component
358 regulatory systems are also commonly implicated in this lifestyle transition, and in agreement
359 with this model, 19 mutations in 14 genes encoding sensor kinases, response regulators, or
360 hybrid complexes were identified (Table 3, Table S3). Likewise, nine different nonsynonymous
361 or indel mutations affecting motility and attachment (e.g. *flgB/G, fliC/H/M, pilB/pilQ,* and *cupB3*)
362 were selected in both biofilm and planktonic populations, indicating advantages of disrupting
363 these processes in both lifestyles.
364 More surprising, the most common functional classification of mutated genes was
365 transporters. Nine transporters were mutated repeatedly including: *pitA, pntB, nosD, pchF*,
366 PA14_09300, PA14_22650, PA14_45060, PA14_46110, and PA14_47900, and account for
367 24% (43) cases of parallelism (Table3, Table S3). These transporters include genes with known
368 function including inorganic phosphate transporter *pitA* and copper transporter *nosD*, as well as
369 those with unknown substrates including PA14_46110 and PA14_45060. Of all transporters
370 identified, *pitA* was the only one to reach frequencies above 50% in any population. This led us
371 to identify an additional stressor acting on these populations as a byproduct of growth on
372 arginine as a sole carbon source, which is an alkaline pH (pH = 9.2 at 24 hr) caused by the
373 release of ammonia through deamination (Ha et al. 2014). It remains unclear how these
374 mutated transporters produce adaptations, but they could be acting to balance pH or
375 compensate for redox imbalances or changes in proton motive force. In addition, 18 mutations
376 affected genes involved in various metabolic processes, including *argJ*, a key component of
377 arginine biosynthesis expected to be no longer required due to abundant arginine in the growth
378 media, *soxA*, encoding sarcosine oxidase (Willsey and Wargo 2016), and *cobG*, involved in the
379 aerobic pathway of cobalmin (Vitamin B12) biosynthesis (Blanche et al. 1992). Further, three

mutations are observed in each of *napF*, *nqrE*, and *nuoG* potentially altering the energy conserving respiratory NADH dehydrogenase chain (Hoboth et al. 2009). We suspect that many of these nonsynonymous or indel mutations are partial loss of function mutations in metabolic pathways that are extraneous in the M63+arginine medium, though an exact mechanism is unknown.

There are four notable cases of mutated genes that are lifestyle specific. Four genes (*rpoB, gacS*, PA14_71750, and PA14_13150) are only mutated in biofilm populations, and in all cases, mutations rise to greater than 90% in at least one population (Table 3, Table S3). Mutations in *rpoB* and other RNA polymerase genes (*rpoACD*) have been frequently identified as adaptations during evolution experiments (O'Sullivan et al. 2005; Xiao et al. 2017). One explanation in *Escherichia coli* suggests they are adaptive for growth in minimal media by redistributing RNA polymerase from small RNA promoters (i.e. rRNA) to rate-limited promoters required for anabolic processes from a limited set of carbon sources, such as arginine in the case of this study (Conrad et al. 2010). GacS is a sensor/regulator hybrid known to govern a broad range of traits involved in virulence, secondary metabolism and biofilm formation through the regulation of small rRNA's (Gellatly et al. 2018). Further, *gacS* has been shown to be involved in the switch from a hyperadherent small colony phenotype back to a wild type phenotype indicating that loss of GacS function is beneficial in biofilms(Davies et al. 2007). The additional two biofilm specific loci, PA14_13150 and PA14_71750, are less understood transcriptional regulators, however PA14_71750 has been previously associated with biofilm adaptation in *Pseudomonas* (Konikkat et al. 2020).

The rarity of fixation events and the high incidence of genes with parallel mutations throughout the experiment provides further evidence of competition between adaptive lineages in a population, or clonal interference (Lang et al. 2013). Given a set of genes in which mutations are adaptive, we would expect each competing genotype to contain different combinations of these mutations, with the most beneficial of them repeatedly evolving on

different genetic backgrounds. As predicted, we identified 55 cases of within-population gene level parallelism (4 – 16 cases per population), with most (87%) predicted to be on different genotypes. This result also demonstrates the polygenic capacity for adaptation by *P. aeruginosa* growing in minimal arginine medium.

Gene	Total cases	Type			Biofilm	Planktonic	Highest frequency						Function
		NS	S	Indel			B1	B2	B3	P1	P2	P3	
argJ	3	3	0	0	2	1		13.5	10.5			11.4	Arginine biosynthesis
soxA	3	2	1	0	1	2			10.6		14.7	11.4	Carbon compound catabolism
aer2	5	3	2	0	3	2		9.6	10.9	10.2		14.2	Chemotaxis
bdlA	3	3	0	0	3	0	14.4	14.7	13.5				Chemotaxis
cobG	3	2	0	1	1	2		61.8			13.6	13.1	Cofactor biosynthesis
mutS	3	3	0	0	2	1	100	100				52.6	DNA replication
napF	3	3	0	0	2	1	13.8		10.9			10.7	Energy metabolism
nqrE	3	3	0	0	1	2		11.7			10.4	11.2	Energy metabolism
nuoG	3	3	0	0	1	2	12.9			12.1	13.9		Energy metabolism
PA14_53110	7	7	0	0	2	5		14.8	12.8	12.9	14.4	12.1	Putative enzymes
pslI	7	7	0	0	3	4	16.7	16.4	14.6	16	14.7		Putative enzymes
algF	3	3	0	0	2	1	13.1			10.6			Secreted Factors
fha1	4	4	0	0	3	1	27.6		25.1	35.8			Secreted Factors
rpoB	4	4	0	0	4	0	100	66	100				Transcription
PA14_13150	3	3	0	0	3	0	46.3	17.8	100				Transcriptional regulators
PA14_18200	6	6	0	0	5	1	22.3	22.1		12.8			Transcriptional regulators
PA14_51840	3	3	0	0	0	3					12	16.6	Transcriptional regulators
PA14_58510	5	3	2	0	4	1	23	15.7		15.5			Transcriptional regulators
PA14_71750	3	3	0	0	3	0	93.9	89.7					Transcriptional regulators
dsbA2	4	2	2	0	3	1	17.1	11.4	20.8			10.5	Translation
rluB	10	8	2	0	4	6	10.8	17.7			14.7	13.2	Translation
nosD	5	4	1	0	1	4	14.1				15.3	12.9	Transporter
PA14_09300	3	3	0	0	2	1	16		15.2	18.6			Transporter
PA14_22650	7	7	0	0	3	4	43.2	24		40	28	37.8	Transporter
PA14_45060	6	6	0	0	2	4	24.4	19.1		19.5	14.1	13.6	Transporter
PA14_46110	7	7	0	0	1	6			15.5	13.7	13.6	10.7	Transporter
PA14_47900	3	3	0	0	0	3						19.9	Transporter
pchF	3	3	0	0	3	0	18.4		19				Transporter
pitA	4	2	0	2	2	3		91.1		100	75.8	100	Transporter
pntB	5	3	2	0	1	4	11.3				13.9	15.6	Transporter
PA14_10770	3	2	1	0	1	2		100		12.2		26.3	Two-component regulatory systems
PA14_32300	3	3	0	0	2	1	17.1					15.3	Two-component regulatory systems
gacS	3	3	0	0	3	0	85.2	92.2					Two-component regulatory systems
PA14_01160	3	3	0	0	1	2	14.3				13.8		Unknown
PA14_20510	6	6	0	0	3	3	9.6	11.5		11	11.9	11.1	Unknown
PA14_31070	10	5	5	0	4	6	19.3	16.9		16.2	16.9		Unknown
PA14_32830	6	6	0	0	2	4		13.8	12.7	12.1	13.5	12.1	Unknown
PA14_54810	3	3	0	0	3	0	11.7		7.5				Unknown
PA14_58070	6	6	0	0	5	1	13.6	17.5	12.9		20.8		Unknown
PA14_69010	5	5	0	0	3	2	20.1	12.2	13	12.5		12.4	Unknown

Table 2. Genes (n=40) with 3 or more evolved mutations. NS: nonsynonymous, S: synonymous, indel: insertion/deletion. Shading corresponds to frequency. Function from PseudoCap via pseudomonas.com.

Selected genotypes are adapted to both growth conditions and lifestyle

Most cases of gene-level parallelism were shared between biofilm and planktonic conditions and indicate adaptations to the common growth media. However, minority variants could include environment specific adaptations. For example, our bead transfer model simulates the complete life cycle of the biofilm – attachment, assembly, dispersal, and reattachment – each of which could select for discrete phenotypes. To distinguish genotypes adapted to either biofilm or planktonic growth, we grew 90-day samples of evolved populations B1, B2, P1, and P2 for two days in each of these conditions independently (Figure 6). We hypothesized that these treatments would enrich genotypes adapted to either condition that we could resolve by resequencing treated populations and correlating their relative frequencies. Mutation frequencies that are higher in one environment, could represent genotypes that are adapted to biofilm or planktonic growth.

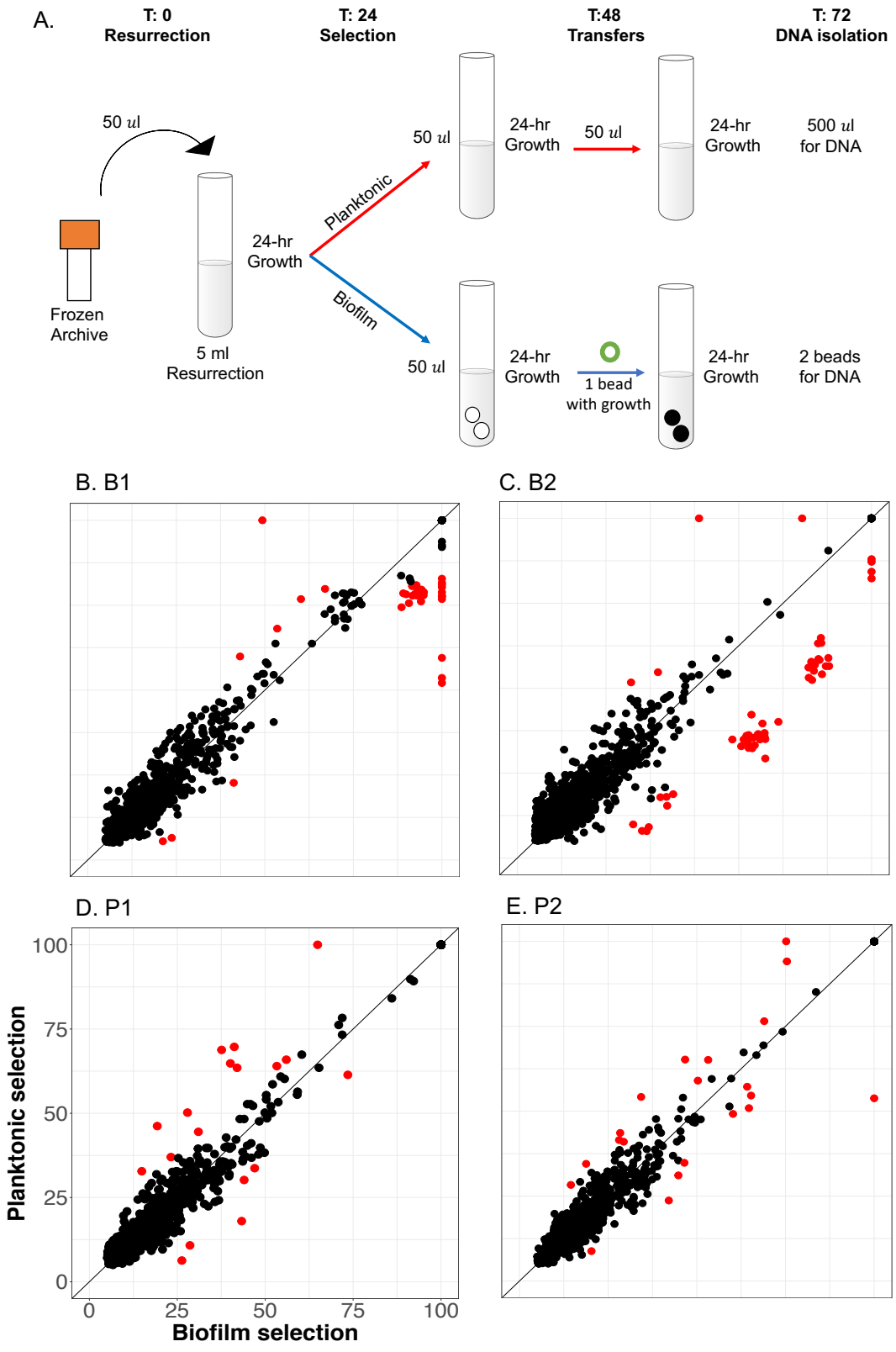

Figure 6. Ecological signals from WGPS data after two days of selection enriches mutations adaptive in both planktonic and biofilm conditions. A. Methods for isolating DNA to identify

genotype by environment interactions. 90-day populations were resurrected from frozen archives in planktonic environments for 24 hours. Each population was then split and subjected to two days of either planktonic selection, via 1:100 daily transfers, or biofilm selection, via the bead model. After the second day of selection, 0.5 ml of planktonic culture and two biofilm beads were used to obtain the planktonic and biofilm DNA samples, respectively (see methods). B-E. Correlation of mutational frequencies when resurrected population DNA is isolated after two days of planktonic selection versus biofilm selection. B: B1 population, C: B2 population, D: P1 population, and E: P2 population. Mutations that are significantly enriched via Cook's distance (see methods) are represented in red and other mutations in black.

In all four populations tested we found significant enrichment in both biofilm and planktonic environments (Figure 6 b-e). As expected, the two biofilm populations tested had more biofilm enriched mutations than planktonic enriched (37 and 55 biofilm enriched compared to 4 and 2 planktonic enriched), though planktonic populations had roughly equal numbers of biofilm and planktonic enriched mutations (8 and 10 biofilm enriched versus 10 and 11 planktonic enriched; Table S4). Upon closer examination, the B2 population appears to contain a set of 36 mutations belonging to 4 genotypes enriched for biofilm fitness (Table S4). These genotypes also rose in frequency between days 75 to 90 in the evolution environment and appear to be generally adaptive. However, these experiments did not generally cause large (>10%) shifts in genotype frequency, which suggests that they correspond to adaptations to the overall experimental conditions and not just these growth phases.

Discussion:

We used experimental evolution to examine how the opportunistic pathogen *Pseudomonas aeruginosa* (PA) adapts in laboratory culture in a medium known to promote biofilm formation (Ha et al. 2014), comparing the results of propagation by simple serial dilution with a model simulating the biofilm life cycle (Poltak and Cooper 2011). After 90 propagations (~600 generations) we observe more mutations per population, fewer fixation events, and earlier prevalence of mutator genotypes than has been observed in other evolution experiments. These findings are consistent with two potentially overlapping processes: 1) the existence of many coexisting niches, representing differing metabolic or ecological strategies within the

462 laboratory environment that select for a variety of specialized genotypes or 2) high clonal
463 interference, involving many genotypes with roughly the same fitness competing against one
464 another in the same niche. The repeated evolution of mutations in the same gene in the same
465 population provides the clearest evidence of this clonal interference, because such mutants are
466 likely to share similar phenotypes. For example, within the B1 population mutations in *gacS*
467 evolve independently in two genotypes (Table S3). We confirmed this finding through clonal
468 sequencing, finding clones H and A to each contain a *gacS* mutation in their distinguishing
469 genotypes (Table 2), and further, these clones were previously shown to compete for a common
470 niche (Flynn et al. 2016). While clonal interference likely contributes to the high genetic variation
471 observed in these populations, we also predict that multiple niches exist within each population
472 as our previous study indicated (Flynn et al. 2016). As further evidence, most cases of gene-
473 level parallel mutations reached only 20-30% frequency within their respective populations
474 (Table 3). We hypothesize that this results from multiple coexisting ecotypes with different
475 adaptations within each population, a phenomenon that has been shown in previous evolution
476 studies, particularly with biofilms (Traverse et al. 2013; Buskirk et al. 2017; Good et al. 2017).
477 To identify the traits selected by growth in a minimal medium containing arginine as sole
478 energy source, we focused on the 40 loci mutated most frequently (Table 2). This medium was
479 selected because it had previously been shown to induce high biofilm production by
480 *Pseudomonas* (Ha et al. 2014) more specifically by increasing intracellular levels of the
481 secondary messenger molecule c-di-GMP through the two diguanylate cyclase proteins RoeA
482 and SadC. Further, arginine was the only amino acid to completely repress swarming motility,
483 indicating this carbon source could be a cue to enter an attached lifestyle (Bernier et al. 2011).
484 As we were interested in seeing how *P. aeruginosa* continues to evolve under conditions where
485 it is already proficient for biofilm, this media choice was suitable. However, it is a naturally
486 stressful environment because arginine catabolism by arginine deiminase produces ammonia
487 as a byproduct and hence an alkaline environment (Cunin et al. 1986; Lu 2006). These

conditions are opposed to previous evolution experiments with *P. aeruginosa* in which media with multiple carbon sources are used to mimic an infection, and the medium often becomes acidic (Bernier et al. 2011; Wong et al. 2012; Ha et al. 2014; Scribner et al. 2019). The exact effects of arginine as the sole carbon and nitrogen source on the metabolic evolution of *P. aeruginosa* are unclear and the topic of a future study, however it is likely that arginine as a sole carbon and nitrogen source produced strong selection and may have been the dominant pressure.

The remarkable, unexpected consequence of this experimental design was a lack of convergent evolution of a small number of genes in replicate populations. Rather, dozens or even hundreds of mutations in nearly as many genes appear to have been selected, suggesting polygenic adaptation involving many metabolic and regulatory systems (Figure 3). Such polygenic selection in large populations increases the probability of clonal interference, wherein each lineage acquires its own combination of adaptations, but any given genotype would struggle to become dominant. Consequently, fixation events were rare, with only ten across all six replicate populations over 600 generations. Further, one of the most commonly mutated pathways was DNA mismatch repair, which increased mutation rates of linked genotypes in the four populations in which they evolved. We hypothesize these mutator genotypes provided the means to escape clonal interference (Good et al. 2014) because they had a higher probability of producing multiple, linked beneficial mutations that could outcompete other genotypes, a phenomenon that has previously been associated with the introduction of alternative forms of structure (Raynes et al. 2019).

Our previous study of these populations predicted that the different colony morphotypes represented lineages that had evolved to occupy distinct, interacting ecological niches within a biofilm population (Flynn et al. 2016). This genomic study confirms that these genotypes indeed represent different long-lived lineages within the B1 population. Each clone was found to possess numerous evolved mutations that are candidates for the observed phenotypic variation

reported previously, e.g. fitness versus the ancestral PA14 strain, levels of cyclic-di-GMP, and motility (Flynn et al. 2016). However, considerably more variation was detected by population sequencing than these lineages could explain, and likewise, sequencing additional clones resulted in an ever-increasing census of new mutations (Figure 4). These results reinforce the polygenic model of adaptation to the biofilm-inducing arginine medium and the diversity of genotypes that can generally improve growth and survival or inhabit the niches illustrated in our prior study (Flynn et al. 2016; Barghi et al. 2020). More generally, this work has implications for understanding processes underpinning the evolution and maintenance of high levels of genetic diversity, including how different nutrient sources influence this process. Although differences in the mode of growth have been shown to influence genetic diversity (O'Toole et al. 2000; Boles et al. 2004; Resch et al. 2005; Booth et al. 2011), the metabolic environment may be equally or even more important by exposing varied fractions of the genome to selection. Further, this study provides a concrete example of how microbial populations evolving in a new environment can adapt and diversify without the periodic losses of genetic variation caused by selective sweeps. This dynamic was demonstrated in the Long-Term Evolution Experiment with *E. coli* after many thousands of generations had passed and the rate of adaptation had slowed (Couce et al. 2017; Good et al. 2017). Yet here, populations amassed extreme fitness gains over only hundreds of generations while maintaining many lineages, suggesting that the *P. aeruginosa* genome encodes vast potential to meet new environmental challenges.

Materials and methods

Experimental evolution

Replicate populations were experimentally evolved as previously reported (Flynn et al, 2016). Briefly, the ancestral *Pseudomonas aeruginosa* (PA14; NC_008463) strain was reconstituted from a freezer stock in Luria-Bertani broth (LB; 1.0% w/v tryptone, 0.5% w/v yeast extract, 1.0% w/v NaCl). Six replicate populations were started with 1:100 dilutions of an

overnight growth into 5 mL M63 media (15 mM $(NH_4)_2SO_4$, 22 mM KH_2PO_4, 40 mM K_2HPO_4, 40 mM galactose, 1 mM $MgSO_4$, 25 μM $FeCl_2$, and 0.4% w/v L-arginine(Bernier et al. 2011)). Three populations were propagated under liquid grown, planktonic, selection (P1, P2, P3), while three populations were propagated, concurrently, under constant biofilm selection (Poltak and Cooper 2011; Traverse et al. 2013; Flynn et al. 2016) (B1, B2, B3). Planktonic selection consisted of daily 1:100 liquid dilutions into 5 mL M63 media, while biofilm selection consisted of the transfer of one 7 mm polystyrene bead every 24 hours to a new tube of 5mL M63 media containing one clean bead. This biofilm selection method requires the entire biofilm lifecycle of dispersal, attachment, and growth between every transfer. All six populations were propagated for 90 days (~600 generations) in 18x150 mm test tubes at 37 °C on a roller drum at 30 rpm.

Archives were made for all populations at days 17, 25, 33, 45, 66, 75, and 90 in 8% dimethyl sulfoxide (DMSO) at -80 °C. Planktonic populations were archived by freezing a 1 ml aliquot of the 24-hour culture, whereas biofilm populations were archived by sonicating 48 hr beads in 1 ml PBS, and then freezing the PBS with 8% DMSO.

Phenotypic characterization of evolved populations

All populations were revived from freezer stocks for characterization by adding 50 μl of freezer stock to a culture of 4:1 M63 media to LB media, with trace elements to recreate previous water mineral content (110.764 g/L $CaCl_2$, 0.824 g/L $MnSO_4$, 33.48 g/L KBr, 132.737 g/L Na_2SiO_3, 123.485 $ZnSO_4$, 0.178 g/L $CoCl_2$ *$6H_2O$, 1.458 g/L $CuSO_4$). This media combination was used to minimize selection effects of growing in a fully complex medium, while providing enough nutrients for the frozen cells to revive. Resurrected populations were grown for 24 hr at 37 °C on a roller drum before being vortexed for 10 seconds, twice, to ensure biofilm growth was disrupted from the sides of the glass tube.

Growth curves were measured for resurrected populations in 96 well plates, at 37 °C. All growth curves were started at an OD_{600} of 0.01 and growth was measured every 10 min

following 9 min of shaking for 24 hr in M63 media with trace elements. Maximum growth rate was determined for the average of all replicates, by using the following equation:

$$r = \frac{\Delta \log (OD600)}{\Delta t}$$

Census population size was calculated by diluting resurrected populations 1:100 in 5 mL M63 media with trace elements. One 7 mm polystyrene bead was added to each biofilm culture at time zero. After 24 hr growth, all populations were vortexed for 30 seconds and then diluted and plated in triplicate on tryptic soy agar and grown at 37 °C for 48 hrs. Average colony counts of the three technical replicates were reported for each population. Additionally, populations plated for census population size were also used for pH measurements as they were complete replications of experimental conditions. Average pH of triplicate readings are reported.

Biofilm assays were performed on resurrected populations diluted to an OD_{600} of 0.01 in M63 media and grown in a 96 well plate under static conditions for 24 hr at 37 °C. Media was discarded and the plate was washed twice with deionized H_2O, which was also discarded. Wells were then stained with the addition of 250 μl 0.1% crystal violet solution for 15 minutes. Plates were rinsed to remove excess dye and the plate was allowed to dry for 24 hours. A de-stain solution (95% ethanol, 4.95% dH_2O, and 0.05% Triton X-100 (fisher bioreagents)) was added to wells (250 μl per well), and, after a 15-minute incubation, was transferred to a new 96 well plate. Crystal violet absorbance readings were measured at 590 nm. Reported values are the average of 21 replicates, done across three plates (7 technical replicates per plate). Data were analyzed with a one-way ANOVA with post hoc Tukey test.

Motility assays were performed as described previously (Ha, et al 2014). Briefly, pipet tips were dipped into resurrected populations and stabbed into motility agar (0.3% agar, 6 g/L Na_2HPO_4, 3 g/L KH_2PO_4, 0.5 g/L NaCl, 0.2% glucose, 0.5% casamino acids, 1 mM $MgSO_4$). Increased or decreased motility was determined for all day 90 evolved populations as the diameter of bacterial growth after 24 hr growth at 37 °C compared to the clonal ancestor.

590 Reported values are the average of 5 replicates. Results were analyzed by one-way ANOVA
591 with post hoc Tukey test.

592 **Mutation rate estimate**

593 Isogenic mutants of biofilm evolved mutator alleles *mutS* T112P and *mutL* D467G were
594 used as reported previously(Flynn et al. 2016). Briefly, the two mutator strains and the PA14
595 ancestor were revived from freezer stocks by streaking on ½ trypic soy agar. After 24 hrs growth
596 individual colonies were used to start 30 replicate 5-ml cultures for each strain. After 24 hrs
597 growth at 37° F on a roller drum, populations were diluted and plated on ½ tryptic soy agar both
598 with and without 1mg/ml Ciprofloxacin as a selective agent. Colonies were counted after a 24
599 hour incubation period on both the antibiotic and non-antibiotic plate. We then calculated the
600 fold change in mutation rate using the maximum likelihood method of Gerrish (2008). We
601 performed measurements for all strains simultaneously to minimize variation. Reported values
602 are the average fold change of all replicates.

603 **Genomic sequencing of evolved metagenomes**

604 DNA was isolated from biofilm populations at 113, 167, 293, 440, 500, and 600
605 generations (17, 25, 44, 66, 75, and 90 days) and from planktonic populations at 113, 293, 500,
606 and 600 generations (17, 44, 66, and 90 days). Culture media for DNA isolation was composed
607 of 4:1 M63 to LB media. DNA was isolated from 1 mL resurrected populations using Qiagen's
608 DNeasy Blood & Tissue Kit. Library construction was done using the Illumina Nextera kit as
609 described previously (Baym 2015). Libraries were sequenced on Illumina's NextSeq 500
610 platform by the Microbial Genome Sequencing Center at the University of Pittsburgh. Between
611 13,545,344 and 46,890,487 reads were obtained for each sample, resulting in coverage of 265x
612 - 860x per sample.

613 **Determining mutational frequencies from sequencing data**

614 Initial metagenomics sequencing efforts of the six populations resulted in 121.2 gbps of
615 2x151 bp sequencing reads, that we trimmed and quality filtered with trimmomatic v0.36 using

default parameters(Bolger et al. 2014). The breseq software package v0.31.0 was used to align the filtered reads to the reference PA14 genome (NCBI's RefSeq database: NC_008463.1) and make polymorphism calls(Barrick et al. 2014). All populations were run using the polymorphism mode of breseq with a sliding window of 5 bp and a quality score cutoff of 10. This analysis was done for every population and every time point sequenced. The genome of the ancestral strain differed from the reference by 435 mutations, which were removed from all evolved population samples before any downstream analysis to remove mutations that did not evolve over the course of the evolution.

All 12,250 resulting mutation calls were filtered in R (v3.5.1, [5]) to require a mutation to be called by at least 3 reads on each strand (positive and negative). Finally, mutations were filtered to remove regions of high polymorphism. Due to the abundance of repetitive regions in the PA14 genome the false positive rate is high. We therefore examined each call using the alignments produced by breseq and excluded mutations with high sequence variation within the 15 bases both upstream and downstream of the called mutation. Mutations were also filtered for known regions of misalignment such as repeat regions before consolidation into time-series tables containing all real mutated loci for each evolved population (Table S1). The resulting 874 mutations were then used as input in the software package LOLIPop Version 0.8.1. using –similarity-cutoff value of 0.1 for P1, P2, P3, and B1 and a --similarity-cutoff of 0.2 for populations B2 and B3. Increased similarity cutoffs increased the amount of mutations that were grouped into a genotype. Types of mutations were broken down by both nucleotide and amino acid mutation for all evolved populations in R. All scripts for the R filtering and analysis are available on github at: https://github.com/KatrinaHarris23/PALTEanalysis

Calculating dN/dS ratios

To determine the dN/dS ratios, first the dN/dS ratio for each of the 64 codons was calculated. The codon usage for the ancestral, PA14, genome was obtained from (http://www.kazusa.or.jp/codon/). The two resulting matrices were multiplied to obtain a neutral

ratio of nonsynonymous to synonymous substitutions (dN/dS ratio) of 2.96 for the ancestral UCBPP-PA14 genome (script for calculating this can be found on github here https://github.com/KatrinaHarris23/PALTEanalysis/blob/master/dnds_calculator). All reported dN/dS ratios are standardized according to this number with the final number reported being a result of the following equation:

$$dN/dS = \frac{\frac{\#nonsynonymous}{\#synonymous}}{2.96}$$

Experimentally determining ecologically enriched mutations

To determine if mutations were specific to the biofilm lifestyle steps of swimming or attaching, we isolated DNA from evolved populations after additional strong selection in two distinct environments (Figure 5). Populations were resurrected from day 90 archives for the B1, B2, P1, and P2 populations by using 50 ul of the frozen stock into 5 ml resurrection media. After 24 hr growth at 37°C each culture was used to inoculate 2 identical 5 ml M63 arginine media cultures. Two 8mm polystyrene beads were added to one replicate, creating movable biofilm, before both inoculated cultures were placed at 37°C. One transfer was performed for all populations at 24 hr. Swimming was selected for by transferring liquid phase growth form replicates with no beads to a new tube with 5 ml M63 arginine media. Additionally, one bead from replicates with beads was rinsed with PBS and subsequently transferred to a fresh tube of 5 ml M63 media with two differently colored beads. After a final 24 hr incubation at 37°C "planktonically enriched" DNA samples were isolated from 0.5 ml liquid phase from replicates without beads. Growth from the two colored beads, first rinsed in PBS, then sonicated in 1 ml PBS was used in total for our "biofilm enriched" DNA sample. DNA was isolated using the Quiagen DNeasy Blood and Tissue kit.

Between 328 - 410x coverage was obtained for all eight samples. Mutations were filtered by removing all ancestral mutations, and only mutations detected by both biofilm and planktonic

samples for a given population were considered. This sequencing effort resulted in 979, 1021, 879, and 876 mutations in the B1, B2, P1 and P2 populations respectively. Relative frequencies of mutations in the two environments were plotted in R using the ggplot2 package (Figure S8; code used in this analysis is found on github https://github.com/KatrinaHarris23/PALTEanalysis/blob/master/201020_ecological_interactions.R).

Clonal sequencing

To acquire clonal DNA, populations were resurrected in 4ml M63 arginine media with 1ml LB and grown for 24 hr at 37 on a roller drum. Populations were then plated on ½ Tsoy plates down to the -6 dilution to isolate individual colonies. After 24 hr growth and 37 followed by 48 hr room temperature growth clones were selected ensuring that all visible colony morphologies were sampled. Colony growth was picked up and used as inoculum for 5 ml LB cultures. After 24 hr at 37 on a roller drum 1 ml of culture was used for archiving (9% DMSO) and 0.5 ml was used for DNA isolation using the DNeasy Blood and tissue kit. Named clones that were reported previously(Flynn et al. 2016) were already archived and archives were used for resurrection directly into 5 ml LB.

DNA sequencing was performed as with population sequencing, but only requiring 30x coverage per sample. All reads were trimmed with trimmomatic, as populations were, and variant calling was performed using Breseq software default settings. As clonal samples are only looking for mutations that fix in each sample, filtering was only performed to remove ancestral mutations before analysis.

Statistical testing

Alpha diversity was calculated for all detected mutations in each population at each time point. We used the “shannon”, “simpson” and “invsimpson”, modes of the diversity function in R. Populations were grouped by growth environment, biofilm (n = 3) and planktonic (n = 3), and by

691 mutator allele presence (n = 4) or absence (n = 2). T-tests were performed in Prism (version 8,
692 www.graphpad.com, Figure S4).
693 To perform the Fisher's exact test, a table of loci observed mutated 2 or more times was
694 generated from the final mutation calls. Locus length was determined using
695 http://pseudomonas.com as either gene length or the distance between surrounding genes for
696 intergenic regions. Fisher's exact test was performed using this compiled list: the numbers of
697 mutations per loci, the total number of mutations observed (624), and the PA14 genome length
698 (6537648). Testing was performed using the fisher.test() function in R and only loci with p-
699 values lower than 0.05 were used for parallelism analysis. 153 loci were tested for parallelism
700 and then the number of false positives were reduced using the Benjamini-Hochberg correction
701 with a false discovery rate of 5%. The equation used was (i/m)Q where i is the p-value rank, m
702 is the total number of tests, and Q is the false discovery rate.
703 Finally, ecological enrichment significance was calculated in R by using Cook's distance.
704 First, a linear regression was calculated for each population using planktonic versus biofilm
705 frequencies using the lm() function. Cook's distance was then calculated for each point, using
706 cooks.distance() function. A mutation was considered significantly enriched if its distance was
707 four times the mean distance or more.
708 **Principal component analysis (PCA)**
709 All PCA calculations and plotting were performed in R. Principal components were
710 computed from the biofilm production, swimming motility, and maximum growth rate (Vmax)
711 data, and from the mutational frequency data at each sampled day using the prcomp() function.
712 Plotting was done using the autoplot() function that is part of the ggfortify package.
713
714 **Acknowledgements**

715 This work was supported by NASA CAN-7 NNA15BB04A and a Research Development Pilot
716 award from the Cystic Fibrosis Foundation to VSC. We thank Dan Snyder and Ann Donnelly for
717 critical feedback and Christopher Deitrick for support in implementing the lolipop package.

718 Bibliography

719 Ashish A, Paterson S, Mowat E, Fothergill JL, Walshaw MJ, Winstanley C. 2013. Extensive
720 diversification is a common feature of Pseudomonas aeruginosa populations during
721 respiratory infections in cystic fibrosis. *J. Cyst. Fibros. Off. J. Eur. Cyst. Fibros. Soc.*
722 12:790–793.

723 Badal D, Jayarani AV, Kollaran MA, Kumar A, Singh V. 2020. Pseudomonas aeruginosa biofilm
724 formation on endotracheal tubes requires multiple two-component systems. *J. Med.*
725 *Microbiol.* 69:906–919.

726 Barghi N, Hermisson J, Schlötterer C. 2020. Polygenic adaptation: a unifying framework to
727 understand positive selection. *Nat. Rev. Genet.* 21:769–781.

728 Barrett RDH, MacLean RC, Bell G. 2005. Experimental Evolution of Pseudomonas fluorescens
729 in Simple and Complex Environments. *Am. Nat.* 166:470–480.

730 Barrick JE, Colburn G, Deatherage DE, Traverse CC, Strand MD, Borges JJ, Knoester DB,
731 Reba A, Meyer AG. 2014. Identifying structural variation in haploid microbial genomes
732 from short-read resequencing data using breseq. *BMC Genomics* 15:1039.

733 Basta DW, Bergkessel M, Newman DK. 2017. Identification of Fitness Determinants during
734 Energy-Limited Growth Arrest in Pseudomonas aeruginosa. *mBio* [Internet] 8. Available
735 from: https://mbio.asm.org/content/8/6/e01170-17

736 Bernier SP, Ha D-G, Khan W, Merritt JH, O'Toole GA. 2011. Modulation of Pseudomonas
737 aeruginosa surface-associated group behaviors by individual amino acids through c-di-
738 GMP signaling. *Res. Microbiol.* 162:680–688.

739 Birky CW, Walsh JB. 1988. Effects of linkage on rates of molecular evolution. *Proc. Natl. Acad.*
740 *Sci.* 85:6414–6418.

741 Blanche F, Famechon A, Thibaut D, Debussche L, Cameron B, Crouzet J. 1992. Biosynthesis of
742 vitamin B12 in Pseudomonas denitrificans: the biosynthetic sequence from precorrin-6y
743 to precorrin-8x is catalyzed by the cobL gene product. *J. Bacteriol.* 174:1050–1052.

744 Boles BR, Thoendel M, Singh PK. 2004. Self-generated diversity produces "insurance effects" in
745 biofilm communities. *Proc. Natl. Acad. Sci.* 101:16630–16635.

746 Bolger AM, Lohse M, Usadel B. 2014. Trimmomatic: a flexible trimmer for Illumina sequence
747 data. *Bioinforma. Oxf. Engl.* 30:2114–2120.

748 Booth SC, Workentine ML, Wen J, Shaykhutdinov R, Vogel HJ, Ceri H, Turner RJ, Weljie AM.
749 2011. Differences in Metabolism between the Biofilm and Planktonic Response to Metal
750 Stress. *J. Proteome Res.* 10:3190–3199.

751 Buskirk SW, Peace RE, Lang GI. 2017. Hitchhiking and epistasis give rise to cohort dynamics in
752 adapting populations. *Proc. Natl. Acad. Sci.* 114:8330–8335.

753 cdeitrick. 2020. cdeitrick/Lolipop. Available from: https://github.com/cdeitrick/Lolipop

754 Ciofu O, Mandsberg LF, Bjarnsholt T, Wassermann T, Høiby N. 2010. Genetic adaptation of
755 Pseudomonas aeruginosa during chronic lung infection of patients with cystic fibrosis:
756 strong and weak mutators with heterogeneous genetic backgrounds emerge in mucA
757 and/or lasR mutants. *Microbiology,* 156:1108–1119.

758 Comeron JM, Williford A, Kliman RM. 2008. The Hill–Robertson effect: evolutionary
759 consequences of weak selection and linkage in finite populations. *Heredity* 100:19–31.

760 Conrad TM, Frazier M, Joyce AR, Cho B-K, Knight EM, Lewis NE, Landick R, Palsson BO.
761 2010. RNA polymerase mutants found through adaptive evolution reprogram
762 Escherichia coli for optimal growth in minimal media. *Proc. Natl. Acad. Sci.* 107:20500–
763 20505.

764 Cooper VS. 2018. Experimental Evolution as a High-Throughput Screen for Genetic
765 Adaptations. *mSphere* 3:e00121-18.

766 Couce A, Caudwell LV, Feinauer C, Hindré T, Feugeas J-P, Weigt M, Lenski RE, Schneider D,
767 Tenaillon O. 2017. Mutator genomes decay, despite sustained fitness gains, in a long-
768 term experiment with bacteria. *Proc. Natl. Acad. Sci.* 114:E9026–E9035.

769 Cunin R, Glansdorff N, Piérard A, Stalon V. 1986. Biosynthesis and metabolism of arginine in
770 bacteria. *Microbiol. Rev.* 50:314–352.

771 Davies JA, Harrison JJ, Marques LLR, Foglia GR, Stremick CA, Storey DG, Turner RJ, Olson
772 ME, Ceri H. 2007. The GacS sensor kinase controls phenotypic reversion of small
773 colony variants isolated from biofilms of Pseudomonas aeruginosa PA14. *FEMS*
774 *Microbiol. Ecol.* 59:32–46.

775 Dietrich LEP, Okegbe C, Price-Whelan A, Sakhtah H, Hunter RC, Newman DK. 2013. Bacterial
776 community morphogenesis is intimately linked to the intracellular redox state. *J.*
777 *Bacteriol.* 195:1371–1380.

778 Eichner A, Günther N, Arnold M, Schobert M, Heesemann J, Hogardt M. 2014. Marker genes
779 for the metabolic adaptation of Pseudomonas aeruginosa to the hypoxic cystic fibrosis
780 lung environment. *Int. J. Med. Microbiol. IJMM* 304:1050–1061.

781 Ellis CN, Schuster BM, Striplin MJ, Jones SH, Whistler CA, Cooper VS. 2012. Influence of
782 seasonality on the genetic diversity of Vibrio parahaemolyticus in New Hampshire
783 shellfish waters as determined by multilocus sequence analysis. *Appl. Environ.*
784 *Microbiol.* 78:3778–3782.

785 Feliziani S, Marvig RL, Luján AM, Moyano AJ, Di Rienzo JA, Krogh Johansen H, Molin S,
786 Smania AM. 2014. Coexistence and Within-Host Evolution of Diversified Lineages of
787 Hypermutable <italic>Pseudomonas aeruginosa</italic> in Long-term Cystic Fibrosis
788 Infections. *PLoS Genet* 10:e1004651.

789 Feliziani S, Marvig RL, Luján AM, Moyano AJ, Rienzo JAD, Johansen HK, Molin S, Smania AM.
790 2014. Coexistence and Within-Host Evolution of Diversified Lineages of Hypermutable
791 Pseudomonas aeruginosa in Long-term Cystic Fibrosis Infections. *PLOS Genet.*
792 10:e1004651.

793 Flynn KM, Dowell G, Johnson TM, Koestler BJ, Waters CM, Cooper VS. 2016. Evolution of
794 Ecological Diversity in Biofilms of Pseudomonas aeruginosa by Altered Cyclic
795 Diguanylate Signaling. *J. Bacteriol.* 198:2608–2618.

796 Francis VI, Stevenson EC, Porter SL. 2017. Two-component systems required for virulence in
797 Pseudomonas aeruginosa. *FEMS Microbiol. Lett.* [Internet] 364. Available from:
798 https://academic.oup.com/femsle/article/364/11/fnx104/3828290

799 Gellatly SL, Bains M, Breidenstein EBM, Strehmel J, Reffuveille F, Taylor PK, Yeung ATY,
800 Overhage J, Hancock REW. 2018. Novel roles for two-component regulatory systems in
801 cytotoxicity and virulence-related properties in Pseudomonas aeruginosa. *AIMS*
802 *Microbiol.* 4:173–191.

803 Gloag ES, Marshall CW, Snyder D, Lewin GR, Harris JS, Santos-Lopez A, Chaney SB,
804 Whiteley M, Cooper VS, Wozniak DJ. 2019. Pseudomonas aeruginosa Interstrain
805 Dynamics and Selection of Hyperbiofilm Mutants during a Chronic Infection. *mBio*
806 [Internet] 10. Available from: https://mbio.asm.org/content/10/4/e01698-19

807 Good BH, McDonald MJ, Barrick JE, Lenski RE, Desai MM. 2017. The Dynamics of Molecular
808 Evolution Over 60,000 Generations. *Nature* 551:45–50.

809 Good BH, Walczak AM, Neher RA, Desai MM. 2014. Genetic Diversity in the Interference
810 Selection Limit. *PLOS Genet.* 10:e1004222.

811 Ha D-G, Richman ME, O'Toole GA. 2014. Deletion Mutant Library for Investigation of Functional
812 Outputs of Cyclic Diguanylate Metabolism in Pseudomonas aeruginosa PA14. *Appl Env.*
813 *Microbiol* 80:3384–3393.

814 Habets MGJL, Rozen DE, Hoekstra RF, de Visser JAGM. 2006. The effect of population
815 structure on the adaptive radiation of microbial populations evolving in spatially
816 structured environments. *Ecol. Lett.* 9:1041–1048.

817 Hoboth C, Hoffmann R, Eichner A, Henke C, Schmoldt S, Imhof A, Heesemann J, Hogardt M.
818 2009. Dynamics of Adaptive Microevolution of Hypermutable Pseudomonas aeruginosa
819 during Chronic Pulmonary Infection in Patients with Cystic Fibrosis. *J. Infect. Dis.*
820 200:118–130.

821 Hogardt M, Heesemann J. 2013. Microevolution of Pseudomonas aeruginosa to a Chronic
822 Pathogen of the Cystic Fibrosis Lung. In: Dobrindt U, Hacker JH, Svanborg C, editors.
823 Between Pathogenicity and Commensalism. Current Topics in Microbiology and
824 Immunology. Berlin, Heidelberg: Springer. p. 91–118. Available from:
825 https://doi.org/10.1007/82_2011_199

826 Junop MS, Yang W, Funchain P, Clendenin W, Miller JH. 2003. In vitro and in vivo studies of
827 MutS, MutL and MutH mutants: correlation of mismatch repair and DNA recombination.
828 *DNA Repair* 2:387–405.

829 Kaczanowska M, Rydén-Aulin M. 2007. Ribosome Biogenesis and the Translation Process in
830 Escherichia coli. *Microbiol. Mol. Biol. Rev. MMBR* 71:477–494.

831 Khademi SMH, Sazinas P, Jelsbak L. 2019. Within-Host Adaptation Mediated by Intergenic
832 Evolution in Pseudomonas aeruginosa. *Genome Biol. Evol.* 11:1385–1397.

833 Kim W, Racimo F, Schluter J, Levy SB, Foster KR. 2014. Importance of positioning for microbial
834 evolution. *Proc. Natl. Acad. Sci. U. S. A.* 111:E1639-1647.

835 Konikkat S, Scribner MR, Eutsey R, Hiller NL, Cooper VS, McManus CJ. 2020. Quantitative
836 mapping of mRNA 3' ends in *Pseudomonas aeruginosa* reveals putative riboregulators
837 and a pervasive role for transcription termination in response to azithromycin.
838 Microbiology Available from: http://biorxiv.org/lookup/doi/10.1101/2020.06.16.155515

839 Krishnan K, Flower AM. 2008. Suppression of ΔbipA Phenotypes in Escherichia coli by
840 Abolishment of Pseudouridylation at Specific Sites on the 23S rRNA. *J. Bacteriol.*
841 190:7675–7683.

842 Kruczek C, Kottapalli KR, Dissanaike S, Dzvova N, Griswold JA, Colmer-Hamood JA, Hamood
843 AN. 2016. Major Transcriptome Changes Accompany the Growth of Pseudomonas
844 aeruginosa in Blood from Patients with Severe Thermal Injuries. *PLOS ONE*
845 11:e0149229.

846 Kryazhimskiy S, Plotkin JB. 2008. The Population Genetics of dN/dS. *PLOS Genet.*
847 4:e1000304.

848 Lang GI, Rice DP, Hickman MJ, Sodergren E, Weinstock GM, Botstein D, Desai MM. 2013.
849 Pervasive Genetic Hitchhiking and Clonal Interference in 40 Evolving Yeast Populations.
850 *Nature* 500:571–574.

851 Lenski RE, Rose MR, Simpson SC, Tadler SC. 1991. Long-Term Experimental Evolution in
852 Escherichia coli. I. Adaptation and Divergence During 2,000 Generations. *Am. Nat.*
853 138:1315–1341.

854 Lieberman TD, Michel J-B, Aingaran M, Potter-Bynoe G, Roux D, Davis MR, Skurnik D, Leiby
855 N, LiPuma JJ, Goldberg JB, et al. 2011. Parallel bacterial evolution within multiple
856 patients identifies candidate pathogenicity genes. *Nat. Genet.* 43:1275–1280.

857 López-Causapé C, Rojo-Molinero E, Mulet X, Cabot G, Moyà B, Figuerola J, Togores B, Pérez
858 JL, Oliver A. 2013. Clonal Dissemination, Emergence of Mutator Lineages and Antibiotic
859 Resistance Evolution in Pseudomonas aeruginosa Cystic Fibrosis Chronic Lung
860 Infection. *PLOS ONE* 8:e71001.

861 Lu C-D. 2006. Pathways and regulation of bacterial arginine metabolism and perspectives for
862 obtaining arginine overproducing strains. *Appl. Microbiol. Biotechnol.* 70:261–272.

863 Macià MD, Pérez JL, Molin S, Oliver A. 2011. Dynamics of Mutator and Antibiotic-Resistant
864 Populations in a Pharmacokinetic/Pharmacodynamic Model of Pseudomonas
865 aeruginosa Biofilm Treatment. *Antimicrob. Agents Chemother.* 55:5230–5237.

866 Martin M, Hölscher T, Dragoš A, Cooper VS, Kovács ÁT. 2016. Laboratory Evolution of
867 Microbial Interactions in Bacterial Biofilms. *J. Bacteriol.* 198:2564–2571.

868 Marvig RL, Dolce D, Sommer LM, Petersen B, Ciofu O, Campana S, Molin S, Taccetti G,
869 Johansen HK. 2015. Within-host microevolution of Pseudomonas aeruginosa in Italian
870 cystic fibrosis patients. *BMC Microbiol.* 15:218.

871 McVean GAT, Charlesworth B. 2000. The Effects of Hill-Robertson Interference Between
872 Weakly Selected Mutations on Patterns of Molecular Evolution and Variation. *Genetics*
873 155:929–944.

874 Morgan R, Kohn S, Hwang S-H, Hassett DJ, Sauer K. 2006. BdlA, a Chemotaxis Regulator
875 Essential for Biofilm Dispersion in Pseudomonas aeruginosa. *J. Bacteriol.* 188:7335–
876 7343.

877 Nicastro GG, Boechat AL, Abe CM, Kaihami GH, Baldini RL. 2009. Pseudomonas aeruginosa
878 PA14 cupD transcription is activated by the RcsB response regulator, but repressed by
879 its putative cognate sensor RcsC. *FEMS Microbiol. Lett.* 301:115–123.

880 O'Sullivan DM, McHugh TD, Gillespie SH. 2005. Analysis of rpoB and pncA mutations in the
881 published literature: an insight into the role of oxidative stress in Mycobacterium
882 tuberculosis evolution? *J. Antimicrob. Chemother.* 55:674–679.

883 O'Toole G, Kaplan HB, Kolter R. 2000. Biofilm Formation as Microbial Development. *Annu. Rev.*
884 *Microbiol.* 54:49–79.

885 Parsek MR, Singh PK. 2003. Bacterial biofilms: an emerging link to disease pathogenesis.
886 *Annu. Rev. Microbiol.* 57:677–701.

887 Periasamy S, Kolenbrander PE. 2009. Mutualistic biofilm communities develop with
888 Porphyromonas gingivalis and initial, early, and late colonizers of enamel. *J. Bacteriol.*
889 191:6804–6811.

890 Petrova OE, Sauer K. 2016. Escaping the biofilm in more than one way: desorption, detachment
891 or dispersion. *Curr. Opin. Microbiol.* 30:67–78.

892 Poltak SR, Cooper VS. 2011. Ecological succession in long-term experimentally evolved
893 biofilms produces synergistic communities. *ISME J.* 5:369–378.

894 Rainey PB, Travisano M. 1998. Adaptive radiation in a heterogeneous environment. *Nature*
895 394:69–72.

896 Raynes Y, Sniegowski PD, Weinreich DM. 2019. Migration promotes mutator alleles in
897 subdivided populations. *Evolution* 73:600–608.

898 Resch A, Rosenstein R, Nerz C, Götz F. 2005. Differential Gene Expression Profiling of
899 Staphylococcus aureus Cultivated under Biofilm and Planktonic Conditions. *Appl.*
900 *Environ. Microbiol.* 71:2663–2676.

901 Santos-Lopez A, Marshall CW, Scribner MR, Snyder DJ, Cooper VS. 2019. Evolutionary
902 pathways to antibiotic resistance are dependent upon environmental structure and
903 bacterial lifestyle.Kirkegaard K, Margolis E, editors. *eLife* 8:e47612.

Sanz-García F, Hernando-Amado S, Martínez JL. 2018. Mutational Evolution of Pseudomonas aeruginosa Resistance to Ribosome-Targeting Antibiotics. *Front. Genet.* [Internet] 9. Available from: https://www.ncbi.nlm.nih.gov/pmc/articles/PMC6200844/

Sawai H, Sugimoto H, Shiro Y, Ishikawa H, Mizutani Y, Aono S. 2012. Structural basis for oxygen sensing and signal transduction of the heme-based sensor protein Aer2 from Pseudomonas aeruginosa. *Chem. Commun.* 48:6523–6525.

Schick A, Kassen R. 2018. Rapid diversification of Pseudomonas aeruginosa in cystic fibrosis lung-like conditions. *Proc. Natl. Acad. Sci.* 115:10714–10719.

Scribner MR, Santos-Lopez A, Marshall CW, Deitrick C, Cooper VS. 2019. Parallel evolution of tobramycin resistance across species and environments. *bioRxiv*:758979.

Shaver AC, Dombrowski PG, Sweeney JY, Treis T, Zappala RM, Sniegowski PD. 2002. Fitness evolution and the rise of mutator alleles in experimental Escherichia coli populations. *Genetics* 162:557–566.

Smith JM, Haigh J. 1974. The hitch-hiking effect of a favourable gene. *Genet. Res.* 23:23–35.

Sniegowski PD, Gerrish PJ, Lenski RE. 1997. Evolution of high mutation rates in experimental populations of E. coli. *Nature* 387:703–705.

Stoodley P, Sauer K, Davies DG, Costerton JW. 2002. Biofilms as complex differentiated communities. *Annu Rev Microbiol* 56:187–209.

Tognon M, Köhler T, Gdaniec BG, Hao Y, Lam JS, Beaume M, Luscher A, Buckling A, van Delden C. 2017. Co-evolution with Staphylococcus aureus leads to lipopolysaccharide alterations in Pseudomonas aeruginosa. *ISME J.* 11:2233–2243.

Traverse CC, Mayo-Smith LM, Poltak SR, Cooper VS. 2013. Tangled bank of experimentally evolved Burkholderia biofilms reflects selection during chronic infections. *Proc. Natl. Acad. Sci. U. S. A.* 110:E250-259.

Turner CB, Marshall CW, Cooper VS. 2018. Parallel genetic adaptation across environments differing in mode of growth or resource availability. *Evol. Lett.* 2:355–367.

Wagner VE, Bushnell D, Passador L, Brooks AI, Iglewski BH. 2003. Microarray Analysis of Pseudomonas aeruginosa Quorum-Sensing Regulons: Effects of Growth Phase and Environment. *J. Bacteriol.* 185:2080–2095.

Warren AE, Boulianne-Larsen CM, Chandler CB, Chiotti K, Kroll E, Miller SR, Taddei F, Sermet-Gaudelus I, Ferroni A, McInnerney K, et al. 2011. Genotypic and Phenotypic Variation in Pseudomonas aeruginosa Reveals Signatures of Secondary Infection and Mutator Activity in Certain Cystic Fibrosis Patients with Chronic Lung Infections. *Infect. Immun.* 79:4802–4818.

Willsey GG, Wargo MJ. 2016. Sarcosine Catabolism in Pseudomonas aeruginosa Is Transcriptionally Regulated by SouR. *J. Bacteriol.* 198:301–310.

940 Winsor GL, Griffiths EJ, Lo R, Dhillon BK, Shay JA, Brinkman FSL. 2016. Enhanced annotations
941 and features for comparing thousands of *Pseudomonas* genomes in the Pseudomonas
942 genome database. *Nucleic Acids Res.* 44:D646–D653.

943 Wong A, Rodrigue N, Kassen R. 2012. Genomics of Adaptation during Experimental Evolution
944 of the Opportunistic Pathogen Pseudomonas aeruginosa. *PLOS Genet.* 8:e1002928.

945 Xiao M, Zhu X, Xu H, Tang J, Liu R, Bi C, Fan F, Zhang X. 2017. A novel point mutation in
946 RpoB improves osmotolerance and succinic acid production in Escherichia coli. *BMC*
947 *Biotechnol.* [Internet] 17. Available from:
948 https://www.ncbi.nlm.nih.gov/pmc/articles/PMC5307762/

949 Yen P, Papin JA. 2017. History of antibiotic adaptation influences microbial evolutionary
950 dynamics during subsequent treatment. *PLoS Biol* 15:e2001586.

951 Yildiz FH, Visick KL. 2009. Vibrio biofilms: so much the same yet so different. *Trends Microbiol.*
952 17:109–118.

953